PHYSICAL REVIEW D **96,** 055042 (2017)

Heavy neutrinos from gluon fusion

Richard Ruiz,[*] Michael Spannowsky,[†] and Philip Waite[‡]

Institute for Particle Physics Phenomenology, Department of Physics, Durham University, Durham DH1 3LE, United Kingdom

(Received 28 June 2017; published 27 September 2017)

Heavy neutrinos, a key prediction of many standard model extensions, remain some of the most searched-for objects at collider experiments. In this context, we revisit the premise that the gluon fusion production mechanism, $gg \to Z^*/h^* \to N\nu_\ell$, is phenomenologically irrelevant at the CERN LHC and report the impact of soft gluon corrections to the production cross section. We resum threshold logarithms up to next-to-next-to-next-to-leading logarithmic accuracy (N^{3}LL), thus capturing the dominant contributions to the inclusive cross section up to next-to-next-to-leading order (N^{2}LO). For $m_N > 150$ GeV and collider energies $\sqrt{s} = 7$–100 TeV, corrections to the Born rates span from $+160\%$ to $+260\%$. At $\sqrt{s} = 14$ TeV, the resummed channel is roughly equal in size to the widely-believed-to-be-dominant charged-current Drell-Yan process and overtakes it outright at $\sqrt{s} \gtrsim 20$–25 TeV. Results are independent of the precise nature/mixing of N and hold generically for other low-scale seesaws. Findings are also expected to hold for other exotic leptons and broken axial-vector currents, particularly as the Z^* contribution identically reduces to that of a pseudoscalar.

DOI: 10.1103/PhysRevD.96.055042

I. INTRODUCTION

In stark contrast to the standard model (SM) of particle physics, neutrinos have nonzero mass, and misaligned flavor and mass eigenstates [1,2]. Hence, the origins of their sub-eV masses and large mixing angles are two of the most pressing open questions in particle physics today. In light of recent evidence for the Higgs mechanism's role in generating charged lepton masses [3,4], we argue that the existence of neutrino Dirac masses comparable to other elementary fermions' Dirac masses is an increasingly likely prospect. If this is the case, then observed neutrino phenomenology can be accommodated by low-scale seesaw mechanisms, such as the inverse [5–7] or linear [8,9] seesaw models.

In such seesaw scenarios, TeV-scale heavy neutrinos' mass eigenstates (N) can couple to electroweak (EW) bosons with sizable [10,11] active-sterile mixing, but at the same time do not decouple from Large Hadron Collider (LHC) phenomenology [12,13] due to their pseudo-Dirac nature. Subsequently, low-scale seesaw mechanisms can be tested at the LHC with $\mathcal{O}(100$–$1000)$ fb^{-1} [14–19], demonstrating the sensitivity and complementarity of collider and oscillation experiments.

Hadron collider investigations of heavy N typically rely on the charged-current (CC) Drell-Yan (DY) process [20], shown in Fig. 1(a) and given by

$$q\bar{q}' \to W^{\pm(*)} \to N\ell^\pm, \qquad q \in \{u, c, d, s, b\}, \tag{1}$$

or the sizable vector boson fusion (VBF) channel [21–24],

$$q\gamma \overset{W\gamma \to N\ell}{\to} N\ell^\pm q'. \tag{2}$$

As seen in Fig. 1(c), VBF is driven by the $W\gamma \to N\ell$ subprocess and receives longitudinal W enhancements for $m_N \gg M_W$ [23]. Notable is the renewed interest [24,25] in the gluon fusion (GF) process [24–27], shown in Fig. 1(b),

$$gg \to Z^*/h^* \to N\nu_\ell. \tag{3}$$

Variants of this process have been studied recently in Refs. [28–34]. While GF proceeds anomalously through off-shell Z^*/h^* bosons and is formally an $\mathcal{O}(\alpha_s^2)$ correction to the neutral-current (NC) DY process, $q\bar{q} \to Z^* \to N\nu_\ell$, the channel's cross section is known to surpass the DY and VBF rates for collider energies $\sqrt{s} \gtrsim 30$–40 TeV [24–26]. At 14 TeV, GF is factors smaller than the DY channels. These conclusions are noteworthy, as they rely on the GF rate at leading-order (LO) accuracy being a good estimate of the total cross section. However, at LO, the GF rates for the SM Higgs boson [35–41], heavy scalars [37], and pseudoscalars [42–44] are greatly underestimated.

In light of this, we report, for the first time, the impact of soft gluon corrections to heavy N production in GF. We resum threshold logarithms up to next-to-next-to-next-to-leading logarithmic accuracy (N^{3}LL). For GF, this captures the leading contributions to the inclusive cross section (σ) up to next-to-next-to-leading order (N^{2}LO) [46]. Our findings have immediate impact on searches at hadron colliders, and thereby challenge the paradigm that GF is phenomenologically irrelevant for the discovery and study of heavy N at the LHC.

[*] richard.ruiz@durham.ac.uk
[†] michael.spannowsky@durham.ac.uk
[‡] p.a.waite@durham.ac.uk

 © 2017 American Physical Society

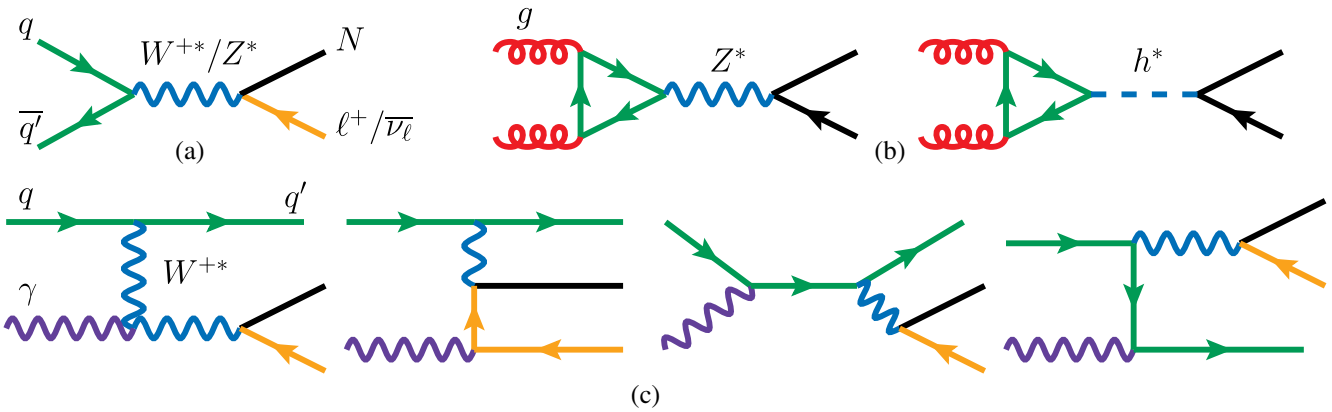

FIG. 1. Born diagrams for heavy N production via the (a) DY, (b) GF, and (c) VBF processes. Drawn using JaxoDraw [45].

For $m_N = 150$–1000 GeV, $\sqrt{s} = 7$–100 TeV, and scale choices comparable to the hard process, we report

$$K^{\mathrm{N^3LL}} = \sigma^{\mathrm{N^3LL}}/\sigma^{\mathrm{LO}}\colon\ 2.6 - 3.6,$$
$$K^{\mathrm{N^2LL}} = \sigma^{\mathrm{N^2LL}}/\sigma^{\mathrm{LO}}\colon\ 2.3 - 3.0. \tag{4}$$

We find that GF dominates over the DY-like processes of Eq. (1) for $m_N = 500$–1000 GeV at $\sqrt{s} \gtrsim 20$–25 TeV. The corrections exhibit perturbative convergence and are consistent with those for Higgs and heavy (pseudo)scalar production [35–44]. Our results are independent of the precise nature/mixing of N and hold generically for other low-scale seesaws. Results are also expected to hold for other exotic leptons—e.g., triplet leptons in the type-III seesaw and other colorless, axial-vector currents.

This report continues as follows: We first describe our phenomenological heavy N model, then present the resummation formalism employed, emphasizing a new treatment of the Z^* current. After summarizing our computational setup, we present our results and conclude.

II. HEAVY NEUTRINO MODEL

Throughout this study, we adopt the neutrino mixing formalism of Ref. [47]: For $i(m) = 1, \ldots, 3$ left-handed (light) states and $j(m') = 1, \ldots, n$ right-handed (heavy) states, chiral neutrinos can be rotated into mass eigenstates by

$$\begin{pmatrix} \nu_{Li} \\ N^c_{Rj} \end{pmatrix} = \begin{pmatrix} U_{3\times 3} & V_{3\times n} \\ X_{n\times 3} & Y_{n\times n} \end{pmatrix} \begin{pmatrix} \nu_m \\ N^c_{m'} \end{pmatrix}. \tag{5}$$

After further rotating the charged leptons into the mass basis, the flavor state ν_ℓ in the mass basis is explicitly

$$\nu_\ell = \sum_{m=1}^{3} U_{\ell m}\nu_m + \sum_{m'=1}^{n} V_{\ell m'} N^c_{m'}. \tag{6}$$

$U_{\ell m}$ is the observed light neutrino mixing matrix, and $V_{\ell m'}$ parametrizes active-heavy mixing. For EW-scale $N_{m'}$, the latter is constrained by precision EW data to be $|V_{\ell N}| \lesssim 10^{-2} - 10^{-1}$ [10,11]. For simplicity, we consider only the lightest heavy state, denoted N.

In the mass basis, the EW interaction Lagrangian is

$$\begin{aligned}\mathcal{L}_{\mathrm{Int}} = &-\frac{g}{\sqrt{2}} W^+_\mu \sum_{\ell=e}^{\tau}\sum_{m=1}^{3} \bar{\nu}_m\, U^*_{\ell m}\gamma^\mu P_L \ell^- \\ &-\frac{g}{\sqrt{2}} W^+_\mu \sum_{\ell=e}^{\tau} \bar{N}^c\, V^*_{\ell N}\gamma^\mu P_L \ell^- \\ &-\frac{g}{2\cos\theta_W} Z_\mu \sum_{\ell=e}^{\tau}\sum_{m=1}^{3} \bar{\nu}_m\, U^*_{\ell m}\gamma^\mu P_L \nu_\ell \\ &-\frac{g}{2\cos\theta_W} Z_\mu \sum_{\ell=e}^{\tau} \bar{N}^c\, V^*_{\ell N}\gamma^\mu P_L \nu_\ell \\ &-\frac{g m_N}{2M_W} h \sum_{\ell=e}^{\tau} \bar{N}^c\, V^*_{\ell N} P_L \nu_\ell + \mathrm{H.c.}\end{aligned} \tag{7}$$

At the production level, $|V_{\ell N}|$ factorizes out of cross sections, a result that holds at all orders in α_s [24,48]. This allows one to define [49] a "bare" cross section σ_0 in which one sets $|V_{\ell N}| = 1$. Subsequently, flavor-model-independent cross sections are given by

$$\sigma(pp \to N + X)/|V_{\ell N}|^2 = \sigma_0(pp \to N + X). \tag{8}$$

Due to this factorization, the QCD corrections we present are universal across low-scale seesaws that feature N.

III. THRESHOLD RESUMMATION FORMALISM

We now summarize our resummation formalism and the special consideration of the Z^* mediator in GF.

For a color-singlet final state V, the inclusive $pp \to V + X$ fixed-order (FO) cross section is given generically by the collinear factorization theorem[1] [50–52],

[1]The equivalent measure, $\int_{\tau_0}^1 d\xi_1 \int_{\tau_0/\xi_1}^1 dx \int_x^1 dz/z$, with $\xi_2 = x/z$, may lead to faster numerical convergence for some processes.

$$\sigma^{\rm FO} = f \otimes f \otimes \Delta \otimes \hat{\sigma} \tag{9}$$

$$= \frac{1}{1+\delta_{ij}} \sum_{i,j,\beta} \int_{\tau_0}^1 d\tau \int_\tau^1 \frac{d\xi_1}{\xi_1} \int_{\tau/\xi_1}^1 \frac{dz}{z} \times [f_{i/p}(\xi_1) f_{j/p}(\xi_2) + (1 \leftrightarrow 2)] \Delta_{ij}^{\beta,\rm FO}(z) \hat{\sigma}_{ij}^{\beta}. \tag{10}$$

That is, the hadronic scattering rate σ is the convolution ($\otimes$) of parton distribution functions (PDFs) f, the soft coefficient function Δ, and the partonic-level $ij \to V$ hard scattering rate $\hat{\sigma}$, which occurs at the hard scattering scale $Q = \sqrt{p_V^2}$. Scale dependence of these quantities is implied but made explicit below. $f_{i/p}(\xi, \mu_f)$ are the likelihoods of observing parton i in p carrying longitudinal momentum $p_z^i = \xi p_z^p \gg p_T^i$, when DGLAP-evolved [53–55] to a factorization scale μ_f, generating the partonic scale $\sqrt{\hat{s}} = \sqrt{\xi_1 \xi_2 s}$. $\Delta_{ij}^{\beta,\rm FO}(z) = \delta(1-z) + \mathcal{O}(\alpha_s)$ accounts for soft gluons carrying a momentum fraction $(1-z)$, with $z = Q^2/\hat{s}$, emitted in the $ij \to A$ transition ($\hat{\sigma}^\beta$) via a color/Lorentz structure labeled as β. Above, $\tau_0 = \min\{Q^2\}/s$ is the kinematic threshold below which $ij \to A$ is kinematically forbidden, and $\tau = Q^2/s = \xi_1 \xi_2 z$ is similarly the hard threshold.

For the $gg \to Z^*/h^* \to N\nu_\ell$ process, with $\beta \in \{Z, h\}$, $Q^2 = (p_N + p_\nu)^2 > m_h^2, M_Z^2$ and $\tau_0 \approx m_N^2/s$, the hard partonic-level Born cross sections are[2] [25,26]

$$\hat{\sigma}^Z = G_F^2 \frac{\alpha_s^2(\mu_r) |V_{\ell N}|^2}{2^4 (4\pi)^3} m_N^2 (1-r_N)^2 |F_Z(Q^2)|^2, \tag{11}$$

$$\hat{\sigma}^h = G_F^2 \frac{\alpha_s^2(\mu_r) |V_{\ell N}|^2}{2^4 (4\pi)^3} \frac{m_N^2 Q^4 (1-r_N)^2}{(Q^2 - m_h^2)^2} |F_h(Q^2)|^2, \tag{12}$$

where $r_X = m_X^2/Q^2$. For quarks with weak isospin charge $(T_L^3)_q = \pm 1/2$, the Z/h one-loop form factors are

$$F_Z(Q^2) = \sum_{q=t,b\ldots} 2(T_L^3)_q [1 - 2 r_q f(r_q)], \tag{13}$$

$$F_h(Q^2) = \sum_{q=t,b\ldots} 2 r_q [2 + (1-4r_q) f(r_q)], \quad \text{with} \tag{14}$$

$$f(r) = \begin{cases} 2\left(\sin^{-1}\frac{1}{2\sqrt{r}}\right)^2, & r > \frac{1}{4}, \\ -\frac{1}{2}\left[\log\left(\frac{1+\sqrt{1-4r}}{1-\sqrt{1-4r}}\right) - i\pi\right]^2, & r \le \frac{1}{4}. \end{cases} \tag{15}$$

A few remarks: (i) While we use the fully integrated $\hat{\sigma}^\beta$, the resummation formalism we employ [56,57] operates in momentum space. Hence, phase-space cuts on an n-body final state can be implemented if one starts from the differential $d\hat{\sigma}^\beta$. (ii) The Z^*/h^* contributions add incoherently due to the (anti)symmetric nature of the $(Z^*)h^*$ coupling [26]. (iii) The similarity of $\hat{\sigma}^Z$ and $\hat{\sigma}^h$ follows from the fact that, after summing over $\mathrm{SU}(2)_L$ doublet constituents, the net Z^* contribution is a pseudoscalar-like coupling proportional to quark Yukawa couplings. This is in accordance with the Goldstone equivalence theorem, pointed out first for the $gg \to N\nu$ process in Ref. [24]. Subsequently, this asymptotic behavior means one can further simplify the original expressions of Refs. [25,26] to those above.

The axial-vector-pseudoscalar correspondence, however, is more general: For a massive, colorless vector $V(q_\mu)$ participating in the loop process $gg \to V^*$, the most general current-propagator contraction (in the unitary gauge) is of the form $\Gamma^\mu \Pi_{\mu\nu} \sim (g_V \gamma^\mu + g_A \gamma^\mu \gamma^5)(g_{\mu\nu} - q_\mu q_\nu / M_V^2)$. By C-symmetry (Furry's theorem), the vector current $g_V \gamma^\mu$ vanishes; by angular momentum conservation (Landau-Yang theorem), the transverse polarization $g_{\mu\nu}$ does not contribute. Hence, $\Gamma^\mu \Pi_{\mu\nu} \sim g_A \gamma^\mu \gamma^5 q_\mu q_\nu / M_V^2$. After decomposing quark propagators in the triangle loop via spinor completeness relations and exploiting the Dirac equation, one finds $\Gamma^\mu \Pi_{\mu\nu} \sim \gamma^5 (2 m_f q_\nu / M_V^2)$—that is, a pseudoscalar coupling proportional to the quark mass m_f.

Moreover, emissions of soft gluons off fermions do not change the loop's structure due to soft factorization. Therefore, one may approximate soft QCD corrections to the $gg \to V^*$ subprocess for V^* possessing axial-vector couplings to fermions with those corrections for a pseudoscalar. This is a main finding of this work and was not observed in previous resummations of $gg \to Z^*$.

As Q approaches the partonic threshold $\sqrt{\hat{s}}$, accompanying gluon radiation is forced to be soft, with $E_g \sim \sqrt{\hat{s}}(1-z)$. This generates numerically large phase-space logarithms of the form $\log(1-z)$ that spoil the perturbative convergence of Eq. (10). Threshold logarithms, however, factorize and can be resummed to all orders in $\alpha_s \log(1-z)$ via exponentiation [58–62].

We perform this resummation by working in the soft-collinear effective theory (SCET) framework [63–65]. This permits Eq. (10) to be factorized directly in momentum space [56,57] by segmenting and regulating divergent regions of phase space with hard and soft scales, μ_h and μ_s. (This is unlike perturbative QCD, where one works in Mellin space [58–60].) Scale invariance of physical observables then implies that factored components can also be independently renormalization-group (RG)-evolved and matched via exponentiation [58–62]. Thus, numerically large quantities are replaced with perturbative ones regulated by μ_h and μ_s and with RG-evolution coefficients that run μ_h and μ_s to μ_f and Q.

In practice, the resummation procedure reduces to replacing the soft coefficient function $\Delta_{ij}^{\beta,\rm FO}(z)$ in Eq. (10):

$$\sigma^{\rm FO} \to \sigma^{\rm Res}\colon\ \Delta_{ij}^{\beta,\rm FO}(z) \to \Delta_{ij}^{\beta,\rm Res}(z). \tag{16}$$

[2]We note that the expression for $\hat{\sigma}^h$ in Ref. [25] contains typographic errors.

For GF production of heavy leptons via s-channel pseudoscalar ($\beta = Z$) and scalar ($\beta = h$) mediators, as given in Fig. 1(b), the SCET-based soft coefficient $\Delta_{gg}^{\beta,\mathrm{Res}}$ in the notation of Refs. [66,67] is

$$\Delta_{gg}^{\beta,\mathrm{Res}}(z) = |C_\beta(Q^2,\mu_h^2)|^2 U(Q^2,\mu_\alpha^2,\mu_h^2,\mu_s^2,\mu_f^2)\frac{\sqrt{z}z^{-\eta}}{(1-z)^{1-2\eta}} \times \tilde{s}_{\mathrm{Higgs}}\left(\log\frac{Q^2(1-z)^2}{\mu_s^2 z} + \partial_\eta, \mu_s\right)\frac{e^{-2\gamma_E\eta}}{\Gamma(2\eta)}. \tag{17}$$

C_β is the process-dependent, so-called hard function and accounts for (hard) virtual corrections to the hard process. For $\beta = h$, the function is given by the two-step SCET matching coefficients C_t and C_S of Ref. [67], with

$$C_h(Q^2,\mu_h^2) \equiv C_t(m_t^2,\mu_t^2)C_S(-Q^2,\mu_h^2), \quad \text{and} \tag{18}$$

$$C_X(Q^2,\mu^2) = \sum_{n=0}^{\infty} C_X^{(n)}(Q^2,\mu^2)\left(\frac{\alpha_s(\mu)}{4\pi}\right)^n, \tag{19}$$

where $X \in \{t, S\}$. The product of C_t and C_S, which can be expanded individually as power series in $(\alpha_s/4\pi)$, is equivalent to a one-step SCET matching procedure when setting $\mu_t = \mu_h$ [68]. For $\beta = Z$, the one-step matching hard function can also be expanded as a power series. In the notation of Refs. [44,69], this is

$$C_Z(Q^2,\mu_h^2) \equiv C_g^{A,\mathrm{eff}}(Q^2,\mu_h^2) = \sum_{n=0}^{\infty} C_{g,n}^{A,\mathrm{eff}}(Q^2,\mu_h^2)\left(\frac{\alpha_s(\mu_h)}{4\pi}\right)^n. \tag{20}$$

We briefly note that the $\log(\mu_h^2/m_t^2)$ term that appears in $C_{g,2}^{A,\mathrm{eff}}$ of Ref. [69] should be replaced with $\log(Q^2/m_t^2)$ in order to preserve the scale independence of the total cross section, a physical observable [44]. With this modification, both C_h and C_Z satisfy the evolution equation,

$$\frac{d}{d\log\mu}C_\beta(Q^2,\mu^2) = \left[\Gamma_{\mathrm{cusp}}^A \log\left(\frac{Q^2}{\mu^2}\right) + \gamma^S + \gamma^t\right]C_\beta(Q^2,\mu^2), \tag{21}$$

for anomalous dimensions $\Gamma_{\mathrm{cusp}}^A, \gamma^{S,t}$, as given in Refs. [66,67].

The soft scalar function $\tilde{s}_{\mathrm{Higgs}}$ describes (soft) radiation off incoming gluons and hence is universal for scalars and pseudoscalars. The derivatives in $\tilde{s}_{\mathrm{Higgs}}$ are regular partial derivatives that act to the right, before $\eta \equiv 2a_\Gamma(\mu_s^2,\mu_f^2)$ is evaluated numerically.

We include an additional factor of $\sqrt{z}$ in Eq. (18) with respect to Refs. [66,67]. As noted in Refs. [66,67,70,71], the inclusion of the factor accounts precisely for power corrections that are manifest in the traditional QCD/Mellin-space resummation formalism. Numerically, we find this increases our total normalization by $\mathcal{O}(5\%\text{–}10\%)$ at N^{3}LL and our residual scale dependence by $\mathcal{O}(5\%)$.

RG running is described by the evolution function,

$$U(Q^2,\mu_\alpha^2,\mu_h^2,\mu_s^2,\mu_f^2) = \frac{\alpha_s^2(\mu_s^2)}{\alpha_s^2(\mu_f^2)}\left[\frac{\beta(\alpha_s(\mu_s^2))/\alpha_s^2(\mu_s^2)}{\beta(\alpha_s(\mu_\alpha^2))/\alpha_s^2(\mu_\alpha^2)}\right]^2\left(\frac{Q^2}{\mu_h^2}\right)^{-2a_\Gamma(\mu_h^2,\mu_s^2)} \times |e^{4\mathcal{S}(\mu_h^2,\mu_s^2)-2a_{\gamma^S}(\mu_h^2,\mu_s^2)+4a_{\gamma^B}(\mu_s^2,\mu_f^2)}|, \tag{22}$$

where $\mu_\alpha = \mu_t(\mu_h)$ for $\beta = h(Z)$.

For definitions and explicit expressions of the quantities in Eqs. (18)–(22) up to $\mathcal{O}(\alpha_s^2)$, see Refs. [66,67]. Mappings between N^{k}LL accuracy and required ingredients can be found in Refs. [66,72]. At N^{3}LL, one needs at two loops C_β for both pseudoscalar [69] and scalar [67,73], as well as $\tilde{s}_{\mathrm{Higgs}}$ [66,67,74]. Note that while the results of Refs. [67,69,73] are derived in the heavy top limit, $\mathcal{O}(Q^2/m_t^2)$ corrections to inclusive (pseudo)scalar cross sections are known to be $\mathcal{O}(1\%\text{–}10\%)$ [37,75], even for $Q^2 \gg m_t^2$, justifying their use in our calculation.

IV. COMPUTATIONAL SETUP

For the DY and VBF channels, we use the methodology of Ref. [24] to compute inclusive cross sections and uncertainties at NLO in QCD, but with the following exceptions: we use the NNPDF 3.0 QED NLO PDF set [76,77] and do not apply phase-space cuts to the CC DY process. Scale choices and regulating VBF cuts are unchanged. For GF, we adopt the additional SM inputs [78]

$$m_b = 0\ \mathrm{GeV}, \quad m_t = 173.2\ \mathrm{GeV}, \quad m_h = 125.7\ \mathrm{GeV}.$$

To best match the accuracy of the resummation calculation, we use the NNPDF 3.0 NNLO + NNLL PDF set [79]; while the set's uncertainties are sizable, the use of a FO PDF set would formally double-count initial-state gluons. Cross sections are calculated using in-house code with Monte Carlo integration performed via the CUBA libraries [80], and checked at LO against Refs. [24,25]. The soft coefficient function $\Delta_{gg}^{\beta,\mathrm{Res}}$ is checked against Refs. [44,72,81].

To minimize the numerical impact of missing QCD corrections, we follow Refs. [66,67] and choose the scale scheme

$$\mu_r, \mu_f, \mu_t, \mu_h = Q \quad \text{and} \quad \mu_s = Q(1-\tau)/(1+7\tau) \tag{23}$$

for both the Born and resummed GF calculations. For GF, we report the scale dependence associated with simultaneously varying μ_f, μ_r, and μ_s over $0.5 \leq \mu_X/\mu_{\mathrm{Default}} \leq 2$. While the μ_s dependence itself is numerically small, we vary it jointly with μ_f to ensure that the subtraction terms required for numerical evaluation lead

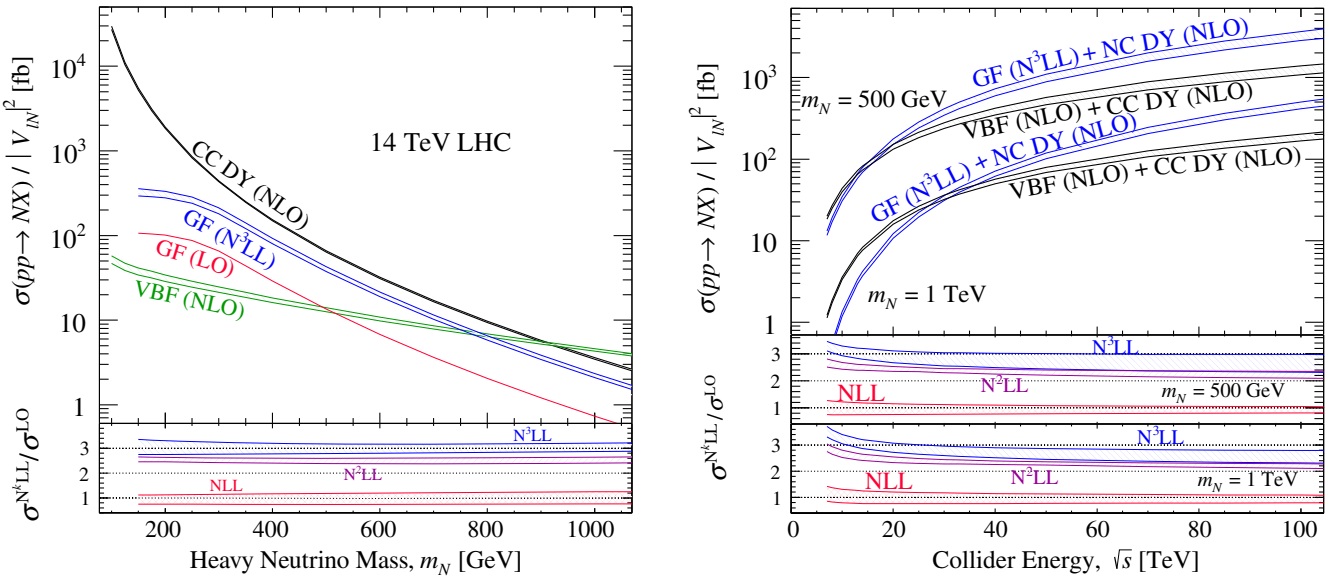

FIG. 2. Heavy N cross sections [fb], divided by the mixing coefficient $|V_{\ell N}|^2$, for various production mechanisms as a function of (left) neutrino mass m_N [GeV] and (right) collider energy [TeV]. Lower: Ratio of the resummed and Born GF predictions.

sufficiently to numerical convergence; see Refs. [66,67] for more details. Missing FO terms that would otherwise stabilize μ_f represents the largest source of uncertainty. Indeed, we find other scale uncertainties to be relatively small, owing to our high logarithmic accuracy.

In the following, we report only residual scale dependence. For studies on PDF uncertainties in heavy N production, see Refs. [23,24], and for threshold-improved PDF uncertainties, see Refs. [82,83]. PDFs and $\alpha_s(\mu)$ are evaluated using the LHAPDF 6 libraries [84].

V. RESULTS

At $\sqrt{s} = 14$ TeV and as a function of heavy N mass, we show in the left plot of Fig. 2 the inclusive N production cross section (divided by active-heavy mixing $|V_{\ell N}|^2$) for the CC DY and VBF processes at NLO, for GF at LO, and for GF at N^{3}LL. The thickness of each curve corresponds to the residual scale dependence; no scale dependence is shown for GF at LO. In the lower panel is the ratio of the resummed and Born GF rates. We quantify the impact of QCD corrections with a K-factor, defined generically as

$$K^{\mathrm{N}^j\mathrm{LO}+\mathrm{N}^k\mathrm{LL}} \equiv \sigma^{\mathrm{N}^j\mathrm{LO}+\mathrm{N}^k\mathrm{LL}}/\sigma^{\mathrm{LO}}. \tag{24}$$

For $m_N = 150$–1000 GeV, cross sections span roughly

$$\text{CC DY NLO: } 3.5\text{–}5400 \text{ fb}, \tag{25}$$

$$\text{GFN}^3\text{LL: } 1.9\text{–}280 \text{ fb}, \tag{26}$$

$$\text{GF LO: } 0.73\text{–}110 \text{ fb}, \tag{27}$$

$$\text{VBF NLO: } 4.4 - 37 \text{ fb}. \tag{28}$$

For GF, K-factors and uncertainties span approximately

$$\text{GF N}^3\text{LL: } K = 3.07\text{–}3.14 \quad \text{with} \quad \delta\sigma/\sigma = \pm 8\%\text{–}13\%, \tag{29}$$

$$\text{GF N}^2\text{LL: } K = 2.59 - 2.66 \quad \text{with} \quad \delta\sigma/\sigma = \pm 6\%\text{–}9\%, \tag{30}$$

$$\text{GF NLL: } K = 1.00\text{–}1.06 \quad \text{with} \quad \delta\sigma/\sigma = \pm 25\%\text{–}27\%. \tag{31}$$

These rates should be compared with DY (VBF) K-factors of $K^{\mathrm{NLO}}_{\mathrm{DY(VBF)}} = 1.15$–$1.25$ $(0.98$–$1.06)$ and uncertainties of $(\delta\sigma/\sigma)^{\mathrm{DY(VBF)}} = \pm 1\%\text{–}5\%(5\%\text{–}11\%)$ [24].

For the mass range under consideration, one observes unambiguously that the resummed GF rates at N^{2}LL and N^{3}LL are markedly larger than the LO rate, with $K \gtrsim 2$–2.5 and notably independent of m_N. This is unlike NLL, where $K \sim 1$, since one essentially runs only $\alpha_s(\mu)$ and C_β, $\tilde{s}_{\mathrm{Higgs}} \sim 1$; here, the uncertainty simply corresponds to varying α_s. We find $\sigma^{\mathrm{N}^3\mathrm{LL}}/\sigma^{\mathrm{N}^2\mathrm{LL}} \sim 1.1$–$1.2$, indicating convergence of the perturbative series.

As previously stated, the residual uncertainty at N^{3}LL stems from missing FO contributions. Such terms, likely positive definite [46], consist of hard, initial-state radiation (ISR) with $p_T^j \gtrsim \mu_f = Q$, which are not, by construction, included in the DGLAP evolution of the PDFs. The sizes of the N^{2}LL and N^{3}LL corrections are, in part, due to our scale choices and the desire to minimize the importance of missing QCD corrections. Choosing alternative, less intuitive scales for the Born process can, of course, lead to smaller K-factors, but also to larger ones. At both N^{2}LL

TABLE I. Heavy N production cross sections via the GF mode at various accuracies, divided by active-heavy mixing $|V_{\ell N}|^2$, scale dependence (%), and K-factor, for representative m_N and $\sqrt{s}$.

$\sqrt{s}$	14 TeV				33 TeV				100 TeV			
m_N	300 GeV		500 GeV		300 GeV		500 GeV		300 GeV		1 TeV	
$\sigma/\lvert V_{\ell N}\rvert^2$ [fb]	σ [fb]	K	σ [fb]	K	σ [fb]	K	σ [fb]	K	σ [fb]	K	σ [fb]	K
GF LO	65.4	⋯	13.5	⋯	415	⋯	115	⋯	2.84×10^3	⋯	154	⋯
GF NLL	$65.9^{+14\%}_{-26\%}$	1.01	$13.7^{+17\%}_{-27\%}$	1.01	$414^{+8\%}_{-23\%}$	1.00	$115^{+11\%}_{-24\%}$	1.00	$2.83^{+2\%}_{-18\%} \times 10^3$	1.00	$154^{+8\%}_{-21\%}$	1.00
GF N^{2}LL	$170^{<1\%}_{-7\%}$	2.61	$34.9^{<1\%}_{-8\%}$	2.59	$1.03^{<1\%}_{-9\%} \times 10^3$	2.49	$281^{<1\%}_{-7\%}$	2.45	$6.83^{+2\%}_{-13\%} \times 10^3$	2.40	$351^{<1\%}_{-8\%}$	2.28
GF N^{3}LL	$202^{+5\%}_{-11\%}$	3.09	$41.3^{+3\%}_{-9\%}$	3.06	$1.21^{+8\%}_{-13\%} \times 10^3$	2.92	$327^{+6\%}_{-11\%}$	2.85	$7.88^{+13\%}_{-16\%} \times 10^3$	2.77	$401^{+8\%}_{-11\%}$	2.60

and N^{3}LL, the size of the uncertainty band is due to a residual μ_f dependence, and requires matching to hard ISR from FO contributions to be reduced. Moreover, these corrections are in line with those for Higgs and heavy (pseudo)scalar production [35–38,41–44].

In comparison with other heavy N production modes, we find for $m_N \gtrsim 300$ GeV that the GF rate is now comparable to the CC and NC DY (not shown for clarity) rates. When basic fiducial cuts are applied on the charged lepton in the CC processes, the combined GF + NC DY rate is slightly larger than the combined VBF + CC DY channel. For $m_N \lesssim 600$ GeV—i.e., masses that are most relevant for LHC phenomenology due to mixing suppression [23,47]—the GF channel is factors larger than the VBF mechanism, indicating its potential importance at the LHC and its upgrades/successors.

We briefly note that the relative importance of the VBF mechanism found in Fig. 2 is considerably less than what has been found in previous investigations—e.g., Ref. [22] and follow-up works by the same authors. It was shown in Ref. [23] that the findings of Ref. [22] were qualitatively and quantitatively incorrect: Their claimed "t-channel enhancement" is in reality several poorly/unregulated QCD and QED collinear divergences. Numerically, their cross sections were overestimated by 100× in some instances. We refer readers to Refs. [23,24,48] for correct, all-orders/resummed treatments of these contributions; to Refs. [15,23] for a quantitative assessment of $W\gamma$ scattering in heavy N searches; and to Ref. [24] for non-expert-friendly infrared- and collinear-safe collider definitions for such processes.

In the right plot of Fig. 2, we plot as a function of $\sqrt{s}$ for representative m_N the summed GF + NC DY channels as well as the summed CC DY + VBF channels. We add the channels incoherently, as GF is formally a noninterfering $\mathcal{O}(\alpha_s^2)$ correction to NC DY, and similarly VBF is a noninterfering $\mathcal{O}(\alpha)$ correction to CC DY. Relative uncertainties are added in quadrature.

We observe for $m_N = 500$–1000 GeV that the *inclusive* production rate of $N\nu$ overtakes the *inclusive* $N\ell^\pm$ production at $\sqrt{s} \gtrsim 15$–30 TeV. For $\sqrt{s} = 33(100)$ TeV, this difference is a factor of $1 - 1.6(2.5$–$2.7)$ and is driven by the GF rate, for which the luminosity grows much faster than the $q\bar{q}'$ (DY) and qq (VBF) luminosities with increasing collider energies. While not shown, we find for $m_N = 500$–1000 GeV that the GF rate individually exceeds the CC DY rate for $\sqrt{s} \gtrsim 20$–25 TeV. For increasing $\sqrt{s}$, we find that the resummation has a smaller impact on the total GF rate, with

$$\text{GF N}^3\text{LL}\colon\ K = 2.6 - 3.6 \quad \text{with} \quad \delta\sigma/\sigma = \pm 8\% - 14\%, \tag{32}$$

$$\text{GF N}^2\text{LL}\colon\ K = 2.3 - 3.0 \quad \text{with} \quad \delta\sigma/\sigma = \pm 6\% - 11\%, \tag{33}$$

$$\text{GF NLL}\colon\ K = 1.0 - 1.2 \quad \text{with} \quad \delta\sigma/\sigma = \pm 19\% - 29\%. \tag{34}$$

This drop in K is again due to an increasing importance of hard ISR, and similarly leads to a sizable residual μ_f dependence. In checks against heavy (pseudo)scalar production [44,72,81], we find similar results, and that the importance of FO corrections is $\mathcal{O}(+10\%)$. Such corrections would likely push net K-factors for the $gg \to N\nu$ process to $K \sim 3$. We summarize our results in Table I.

Due to the severe model-dependence of $V_{\ell N}$ as well as the associated phenomenology, an investigation into which is well beyond the scope of this study, we defer further interpretation of our results to future studies.

Usage: For the use of these results in studies, we advocate LO + parton-shower event generation following Ref. [24]. Total inclusive rates should then be normalized to those tabulated in Tables II and III in the Appendix. The flatness of the resummed K-factors means interpolation to unlisted m_N is reliable.

VI. SUMMARY AND CONCLUSION

The existence of tiny neutrino masses and large mixing is unambiguous evidence for physics beyond the SM. In light of Higgs boson data, the prospect of neutrino Dirac masses existing is increasingly likely. Low-scale seesaw models with TeV-scale heavy neutrinos that couple appreciably to EW bosons are scenarios that can accommodate these seemingly contradictory observations, and still give rise to LHC phenomenology.

In this context, we have evaluated, for the first time, soft corrections to the GF production mode $gg \to Z^*/h^* \to N\nu$. This was made possible by a new treatment of the $gg \to Z^*$ subprocess. For $m_N = 150$–1000 GeV and $\sqrt{s} =$ 7–100 TeV, we report

$$K^{\mathrm{N^3LL}} = \sigma^{\mathrm{N^3LL}}/\sigma^{\mathrm{LO}}\colon\ 2.6 - 3.6, \tag{35}$$

$$K^{\mathrm{N^2LL}} = \sigma^{\mathrm{N^2LL}}/\sigma^{\mathrm{LO}}\colon\ 2.3 - 3.0. \tag{36}$$

We find that GF dominates over DY-like processes of Eq. (1) for $m_N = 500$–1000 GeV at $\sqrt{s} \gtrsim 20$–25 TeV. Corrections exhibit perturbative convergence and are consistent with Higgs and heavy (pseudo)scalar production. Moreover, our results are independent of the precise nature/mixing of N, and are expected to hold for other exotic leptons as well as other colorless, broken axial-vector currents one finds in other seesaw scenarios.

ACKNOWLEDGMENTS

M. Bonvini, S. Dawson, C. Fabrizio, E. Molinaro, B. Pecjak, L. Rottoli, D. Scott, C.-F. Tamarit, and C. Weiland are thanked for discussions. This work was funded in part by the UK STFC, and the European Union's Horizon 2020 research and innovation programme under Marie Sklodowska-Curie Grant Agreement No. 674896 (Elusives ITN). R. R. acknowledges the CERN Theory group's generous hospitality during the completion of this work.

APPENDIX

TABLE II. Total hadronic cross sections for $gg \to Z^*/h^* \to N\nu_\ell$ at various accuracies, divided by active-heavy mixing $|V_{\ell N}|^2$, for representative collider energies $\sqrt{s}$.

m_N [GeV]	$\sigma^{\mathrm{LO}}/\lvert V_{\ell N}\rvert^2$ [fb]	$\sigma^{\mathrm{NLL}}/\lvert V_{\ell N}\rvert^2$ [fb]	$\sigma^{N^2\mathrm{LL}}/\lvert V_{\ell N}\rvert^2$ [fb]	$\sigma^{N^3\mathrm{LL}}/\lvert V_{\ell N}\rvert^2$ [fb]
		$\sqrt{s} = 13$ TeV		
150	$0.9097\mathrm{E}+02$	$0.9131\mathrm{E}+02^{+11.8\%}_{-25.4\%}$	$0.2419\mathrm{E}+03^{+<0.1\%}_{-7.2\%}$	$0.2867\mathrm{E}+03^{+6.5\%}_{-12.3\%}$
175	$0.8811\mathrm{E}+02$	$0.8868\mathrm{E}+02^{+12.4\%}_{-25.8\%}$	$0.2334\mathrm{E}+03^{+<0.1\%}_{-6.8\%}$	$0.2770\mathrm{E}+03^{+5.6\%}_{-12.0\%}$
200	$0.8510\mathrm{E}+02$	$0.8560\mathrm{E}+02^{+12.9\%}_{-25.9\%}$	$0.2243\mathrm{E}+03^{+<0.1\%}_{-6.4\%}$	$0.2665\mathrm{E}+03^{+5.5\%}_{-11.6\%}$
225	$0.8020\mathrm{E}+02$	$0.8075\mathrm{E}+02^{+13.3\%}_{-26.0\%}$	$0.2110\mathrm{E}+03^{+<0.1\%}_{-6.7\%}$	$0.2504\mathrm{E}+03^{+5.2\%}_{-11.3\%}$
250	$0.7330\mathrm{E}+02$	$0.7379\mathrm{E}+02^{+13.7\%}_{-26.2\%}$	$0.1924\mathrm{E}+03^{+<0.1\%}_{-6.9\%}$	$0.2282\mathrm{E}+03^{+5.0\%}_{-11.1\%}$
275	$0.6451\mathrm{E}+02$	$0.6496\mathrm{E}+02^{+14.1\%}_{-26.2\%}$	$0.1690\mathrm{E}+03^{+<0.1\%}_{-7.0\%}$	$0.2008\mathrm{E}+03^{+4.9\%}_{-10.8\%}$
300	$0.5467\mathrm{E}+02$	$0.5507\mathrm{E}+02^{+14.6\%}_{-26.4\%}$	$0.1430\mathrm{E}+03^{+<0.1\%}_{-7.2\%}$	$0.1697\mathrm{E}+03^{+4.6\%}_{-10.4\%}$
325	$0.4500\mathrm{E}+02$	$0.4515\mathrm{E}+02^{+15.0\%}_{-26.3\%}$	$0.1171\mathrm{E}+03^{+<0.1\%}_{-7.2\%}$	$0.1388\mathrm{E}+03^{+4.7\%}_{-10.2\%}$
350	$0.3629\mathrm{E}+02$	$0.3640\mathrm{E}+02^{+15.6\%}_{-26.5\%}$	$0.9423\mathrm{E}+02^{+<0.1\%}_{-7.5\%}$	$0.1117\mathrm{E}+03^{+4.4\%}_{-9.9\%}$
375	$0.2922\mathrm{E}+02$	$0.2947\mathrm{E}+02^{+15.6\%}_{-26.7\%}$	$0.7613\mathrm{E}+02^{+<0.1\%}_{-7.7\%}$	$0.9010\mathrm{E}+02^{+4.2\%}_{-9.7\%}$
400	$0.2370\mathrm{E}+02$	$0.2396\mathrm{E}+02^{+16.1\%}_{-26.7\%}$	$0.6185\mathrm{E}+02^{+<0.1\%}_{-7.8\%}$	$0.7328\mathrm{E}+02^{+3.9\%}_{-9.6\%}$
450	$0.1593\mathrm{E}+02$	$0.1612\mathrm{E}+02^{+16.8\%}_{-27.0\%}$	$0.4147\mathrm{E}+02^{+<0.1\%}_{-8.2\%}$	$0.4910\mathrm{E}+02^{+3.4\%}_{-9.3\%}$
500	$0.1089\mathrm{E}+02$	$0.1106\mathrm{E}+02^{+17.2\%}_{-27.1\%}$	$0.2838\mathrm{E}+02^{+<0.1\%}_{-8.4\%}$	$0.3355\mathrm{E}+02^{+3.4\%}_{-8.9\%}$
550	$0.7617\mathrm{E}+01$	$0.7747\mathrm{E}+01^{+17.5\%}_{-27.3\%}$	$0.1984\mathrm{E}+02^{+<0.1\%}_{-8.6\%}$	$0.2351\mathrm{E}+02^{+3.2\%}_{-8.8\%}$
600	$0.5413\mathrm{E}+01$	$0.5518\mathrm{E}+01^{+18.0\%}_{-27.3\%}$	$0.1410\mathrm{E}+02^{+<0.1\%}_{-8.7\%}$	$0.1670\mathrm{E}+02^{+3.0\%}_{-8.5\%}$
		$\sqrt{s} = 14$ TeV		
150	$0.1065\mathrm{E}+03$	$0.1069\mathrm{E}+03^{+11.2\%}_{-25.0\%}$	$0.2824\mathrm{E}+03^{+<0.1\%}_{-7.5\%}$	$0.3348\mathrm{E}+03^{+6.7\%}_{-12.7\%}$
175	$0.1039\mathrm{E}+03$	$0.1043\mathrm{E}+03^{+11.8\%}_{-25.3\%}$	$0.2733\mathrm{E}+03^{+<0.1\%}_{-7.2\%}$	$0.3239\mathrm{E}+03^{+6.1\%}_{-12.2\%}$
200	$0.1006\mathrm{E}+03$	$0.1012\mathrm{E}+03^{+12.4\%}_{-25.5\%}$	$0.2641\mathrm{E}+03^{+<0.1\%}_{-6.7\%}$	$0.3132\mathrm{E}+03^{+5.7\%}_{-11.9\%}$
225	$0.9522\mathrm{E}+02$	$0.9567\mathrm{E}+02^{+13.0\%}_{-25.7\%}$	$0.2490\mathrm{E}+03^{+<0.1\%}_{-6.3\%}$	$0.2952\mathrm{E}+03^{+5.4\%}_{-11.5\%}$
250	$0.8711\mathrm{E}+02$	$0.8776\mathrm{E}+02^{+13.2\%}_{-25.9\%}$	$0.2279\mathrm{E}+03^{+<0.1\%}_{-6.7\%}$	$0.2702\mathrm{E}+03^{+5.1\%}_{-11.3\%}$
275	$0.7693\mathrm{E}+02$	$0.7746\mathrm{E}+02^{+13.6\%}_{-25.9\%}$	$0.2008\mathrm{E}+03^{+<0.1\%}_{-6.7\%}$	$0.2380\mathrm{E}+03^{+5.1\%}_{-11.0\%}$
300	$0.6538\mathrm{E}+02$	$0.6585\mathrm{E}+02^{+13.9\%}_{-26.0\%}$	$0.1704\mathrm{E}+03^{+<0.1\%}_{-6.8\%}$	$0.2018\mathrm{E}+03^{+5.0\%}_{-10.7\%}$
325	$0.5386\mathrm{E}+02$	$0.5425\mathrm{E}+02^{+14.4\%}_{-26.1\%}$	$0.1401\mathrm{E}+03^{+<0.1\%}_{-7.0\%}$	$0.1659\mathrm{E}+03^{+4.7\%}_{-10.5\%}$
350	$0.4377\mathrm{E}+02$	$0.4395\mathrm{E}+02^{+14.9\%}_{-26.2\%}$	$0.1133\mathrm{E}+03^{+<0.1\%}_{-7.1\%}$	$0.1341\mathrm{E}+03^{+4.6\%}_{-10.2\%}$
375	$0.3557\mathrm{E}+02$	$0.3565\mathrm{E}+02^{+15.5\%}_{-26.2\%}$	$0.9174\mathrm{E}+02^{+<0.1\%}_{-7.2\%}$	$0.1085\mathrm{E}+03^{+4.5\%}_{-9.8\%}$
400	$0.2900\mathrm{E}+02$	$0.2913\mathrm{E}+02^{+15.6\%}_{-26.5\%}$	$0.7480\mathrm{E}+02^{+<0.1\%}_{-7.5\%}$	$0.8841\mathrm{E}+02^{+4.2\%}_{-9.7\%}$
450	$0.1951\mathrm{E}+02$	$0.1975\mathrm{E}+02^{+16.2\%}_{-26.7\%}$	$0.5061\mathrm{E}+02^{+<0.1\%}_{-7.9\%}$	$0.5985\mathrm{E}+02^{+3.8\%}_{-9.5\%}$
500	$0.1351\mathrm{E}+02$	$0.1367\mathrm{E}+02^{+16.8\%}_{-26.9\%}$	$0.3493\mathrm{E}+02^{+<0.1\%}_{-8.1\%}$	$0.4128\mathrm{E}+02^{+3.4\%}_{-9.2\%}$
550	$0.9494\mathrm{E}+01$	$0.9636\mathrm{E}+01^{+17.2\%}_{-27.0\%}$	$0.2456\mathrm{E}+02^{+<0.1\%}_{-8.3\%}$	$0.2899\mathrm{E}+02^{+3.5\%}_{-8.8\%}$
600	$0.6807\mathrm{E}+01$	$0.6922\mathrm{E}+01^{+17.4\%}_{-27.1\%}$	$0.1762\mathrm{E}+02^{+<0.1\%}_{-8.5\%}$	$0.2083\mathrm{E}+02^{+3.2\%}_{-8.7\%}$

TABLE III. Total hadronic cross sections for $gg \to Z^*/h^* \to N\nu_\ell$ at various accuracies, divided by active-heavy mixing $|V_{\ell N}|^2$, for representative collider energies $\sqrt{s}$.

m_N [GeV]	$\sigma^{\rm LO}/\lvert V_{\ell N}\rvert^2$ [fb]	$\sigma^{\rm NLL}/\lvert V_{\ell N}\rvert^2$ [fb]	$\sigma^{N^2{\rm LL}}/\lvert V_{\ell N}\rvert^2$ [fb]	$\sigma^{N^3{\rm LL}}/\lvert V_{\ell N}\rvert^2$ [fb]
		$\sqrt{s} = 33$ TeV		
150	$0.5547\text{E}+03$	$0.5510\text{E}+03^{+5.8\%}_{-21.3\%}$	$0.1408\text{E}+04^{+<0.1\%}_{-10.8\%}$	$0.1658\text{E}+04^{+10.3\%}_{-15.1\%}$
200	$0.5672\text{E}+03$	$0.5663\text{E}+03^{+6.3\%}_{-21.9\%}$	$0.1428\text{E}+04^{+<0.1\%}_{-10.2\%}$	$0.1674\text{E}+04^{+9.7\%}_{-14.1\%}$
300	$0.4146\text{E}+03$	$0.4144\text{E}+03^{+8.3\%}_{-22.5\%}$	$0.1033\text{E}+04^{+<0.1\%}_{-8.8\%}$	$0.1209\text{E}+04^{+8.3\%}_{-13.1\%}$
400	$0.2132\text{E}+03$	$0.2127\text{E}+03^{+10.0\%}_{-23.1\%}$	$0.5250\text{E}+03^{+<0.1\%}_{-7.4\%}$	$0.6134\text{E}+03^{+7.1\%}_{-11.9\%}$
500	$0.1147\text{E}+03$	$0.1146\text{E}+03^{+11.1\%}_{-23.6\%}$	$0.2806\text{E}+03^{+<0.1\%}_{-6.6\%}$	$0.3273\text{E}+03^{+6.3\%}_{-11.1\%}$
600	$0.6606\text{E}+02$	$0.6615\text{E}+02^{+12.0\%}_{-23.9\%}$	$0.1608\text{E}+03^{+<0.1\%}_{-5.9\%}$	$0.1873\text{E}+03^{+5.6\%}_{-10.5\%}$
700	$0.4011\text{E}+02$	$0.4025\text{E}+02^{+13.0\%}_{-24.2\%}$	$0.9747\text{E}+02^{+<0.1\%}_{-5.5\%}$	$0.1135\text{E}+03^{+5.2\%}_{-9.9\%}$
800	$0.2550\text{E}+02$	$0.2564\text{E}+02^{+13.6\%}_{-24.4\%}$	$0.6183\text{E}+02^{+<0.1\%}_{-5.9\%}$	$0.7191\text{E}+02^{+4.8\%}_{-9.5\%}$
900	$0.1681\text{E}+02$	$0.1690\text{E}+02^{+14.2\%}_{-24.7\%}$	$0.4066\text{E}+02^{+<0.1\%}_{-6.3\%}$	$0.4733\text{E}+02^{+4.4\%}_{-9.3\%}$
1000	$0.1141\text{E}+02$	$0.1147\text{E}+02^{+14.8\%}_{-24.7\%}$	$0.2753\text{E}+02^{+<0.1\%}_{-6.4\%}$	$0.3204\text{E}+02^{+4.2\%}_{-9.0\%}$
1100	$0.7916\text{E}+01$	$0.7981\text{E}+01^{+15.2\%}_{-24.9\%}$	$0.1912\text{E}+02^{+<0.1\%}_{-6.6\%}$	$0.2228\text{E}+02^{+4.0\%}_{-8.7\%}$
1200	$0.5625\text{E}+01$	$0.5685\text{E}+01^{+15.4\%}_{-25.0\%}$	$0.1360\text{E}+02^{+<0.1\%}_{-6.8\%}$	$0.1582\text{E}+02^{+3.8\%}_{-8.6\%}$
1300	$0.4066\text{E}+01$	$0.4115\text{E}+01^{+15.8\%}_{-25.1\%}$	$0.9831\text{E}+01^{+<0.1\%}_{-7.0\%}$	$0.1144\text{E}+02^{+3.7\%}_{-8.4\%}$
1400	$0.2985\text{E}+01$	$0.3031\text{E}+01^{+16.0\%}_{-25.2\%}$	$0.7234\text{E}+01^{+<0.1\%}_{-7.1\%}$	$0.8425\text{E}+01^{+3.4\%}_{-8.4\%}$
1500	$0.2225\text{E}+01$	$0.2261\text{E}+01^{+16.3\%}_{-25.2\%}$	$0.5389\text{E}+01^{+<0.1\%}_{-7.1\%}$	$0.6281\text{E}+01^{+3.5\%}_{-8.2\%}$
		$\sqrt{s} = 100$ TeV		
150	$0.3230\text{E}+04$	$0.3223\text{E}+04^{+<0.1\%}_{-16.8\%}$	$0.7967\text{E}+04^{+3.9\%}_{-15.5\%}$	$0.9244\text{E}+04^{+15.2\%}_{-18.8\%}$
200	$0.3516\text{E}+04$	$0.3507\text{E}+04^{+0.1\%}_{-17.2\%}$	$0.8569\text{E}+04^{+3.2\%}_{-14.3\%}$	$0.9922\text{E}+04^{+14.1\%}_{-17.6\%}$
300	$0.2839\text{E}+04$	$0.2832\text{E}+04^{+1.8\%}_{-17.9\%}$	$0.6825\text{E}+04^{+2.2\%}_{-12.9\%}$	$0.7876\text{E}+04^{+13.0\%}_{-16.2\%}$
400	$0.1648\text{E}+04$	$0.1645\text{E}+04^{+3.3\%}_{-18.7\%}$	$0.3909\text{E}+04^{+1.0\%}_{-11.6\%}$	$0.4493\text{E}+04^{+11.6\%}_{-15.0\%}$
500	$0.9911\text{E}+03$	$0.9913\text{E}+03^{+4.7\%}_{-19.2\%}$	$0.2330\text{E}+04^{+0.2\%}_{-10.5\%}$	$0.2674\text{E}+04^{+10.5\%}_{-14.0\%}$
600	$0.6330\text{E}+03$	$0.6322\text{E}+03^{+5.7\%}_{-19.7\%}$	$0.1473\text{E}+04^{+<0.1\%}_{-9.6\%}$	$0.1688\text{E}+04^{+9.8\%}_{-13.1\%}$
700	$0.4242\text{E}+03$	$0.4220\text{E}+03^{+6.6\%}_{-20.0\%}$	$0.9775\text{E}+03^{+<0.1\%}_{-8.9\%}$	$0.1119\text{E}+04^{+9.0\%}_{-12.6\%}$
800	$0.2937\text{E}+03$	$0.2938\text{E}+03^{+7.3\%}_{-20.4\%}$	$0.6768\text{E}+03^{+<0.1\%}_{-8.4\%}$	$0.7728\text{E}+03^{+8.3\%}_{-11.9\%}$
900	$0.2101\text{E}+03$	$0.2101\text{E}+03^{+7.8\%}_{-20.5\%}$	$0.4817\text{E}+03^{+<0.1\%}_{-8.0\%}$	$0.5498\text{E}+03^{+8.1\%}_{-11.6\%}$
1000	$0.1541\text{E}+03$	$0.1538\text{E}+03^{+8.4\%}_{-20.8\%}$	$0.3513\text{E}+03^{+<0.1\%}_{-7.5\%}$	$0.4010\text{E}+03^{+7.8\%}_{-11.2\%}$
1100	$0.1152\text{E}+03$	$0.1153\text{E}+03^{+9.0\%}_{-21.0\%}$	$0.2624\text{E}+03^{+<0.1\%}_{-7.1\%}$	$0.2996\text{E}+03^{+7.5\%}_{-10.9\%}$
1200	$0.8800\text{E}+02$	$0.8830\text{E}+02^{+9.1\%}_{-21.3\%}$	$0.2006\text{E}+03^{+<0.1\%}_{-7.1\%}$	$0.2291\text{E}+03^{+6.9\%}_{-11.0\%}$
1300	$0.6822\text{E}+02$	$0.6839\text{E}+02^{+9.8\%}_{-21.4\%}$	$0.1550\text{E}+03^{+<0.1\%}_{-6.5\%}$	$0.1771\text{E}+03^{+6.6\%}_{-10.4\%}$
1400	$0.5369\text{E}+02$	$0.5371\text{E}+02^{+10.1\%}_{-21.5\%}$	$0.1214\text{E}+03^{+<0.1\%}_{-6.2\%}$	$0.1384\text{E}+03^{+6.6\%}_{-10.1\%}$
1500	$0.4272\text{E}+02$	$0.4278\text{E}+02^{+10.4\%}_{-21.7\%}$	$0.9653\text{E}+02^{+<0.1\%}_{-6.0\%}$	$0.1102\text{E}+03^{+6.2\%}_{-10.1\%}$

[1] Q. R. Ahmad *et al.* (SNO Collaboration), Direct Evidence for Neutrino Flavor Transformation from Neutral Current Interactions in the Sudbury Neutrino Observatory, Phys. Rev. Lett. **89**, 011301 (2002).

[2] Y. Ashie *et al.* (Super-Kamiokande Collaboration), A Measurement of atmospheric neutrino oscillation parameters by Super-Kamiokande I, Phys. Rev. D **71**, 112005 (2005).

[3] S. Chatrchyan *et al.* (CMS Collaboration), Evidence for the 125 GeV Higgs boson decaying to a pair of τ leptons, J. High Energy Phys. 05 (2014) 104.

[4] G. Aad *et al.* (ATLAS Collaboration), Evidence for the Higgs-boson Yukawa coupling to tau leptons with the ATLAS detector, J. High Energy Phys. 04 (2015) 117.

[5] R. N. Mohapatra, Mechanism for Understanding Small Neutrino Mass in Superstring Theories, Phys. Rev. Lett. **56**, 561 (1986).

[6] R. N. Mohapatra and J. W. F. Valle, Neutrino mass and baryon number nonconservation in superstring models, Phys. Rev. D **34**, 1642 (1986).

[7] J. Bernabeu, A. Santamaria, J. Vidal, A. Mendez, and J. W. F. Valle, Lepton flavor nonconservation at high-energies in a superstring inspired standard model, Phys. Lett. B **187**, 303 (1987).

[8] E. K. Akhmedov, M. Lindner, E. Schnapka, and J. W. F. Valle, Left-right symmetry breaking in NJL approach, Phys. Lett. B **368**, 270 (1996).
[9] E. K. Akhmedov, M. Lindner, E. Schnapka, and J. W. F. Valle, Dynamical left-right symmetry breaking, Phys. Rev. D **53**, 2752 (1996).
[10] S. Antusch and O. Fischer, Non-unitarity of the leptonic mixing matrix: Present bounds and future sensitivities, J. High Energy Phys. 10 (2014) 094.
[11] E. Fernandez-Martinez, J. Hernandez-Garcia, and J. Lopez-Pavon, Global constraints on heavy neutrino mixing, J. High Energy Phys. 08 (2016) 033.
[12] A. Pilaftsis, Radiatively induced neutrino masses and large Higgs neutrino couplings in the standard model with Majorana fields, Z. Phys. C **55**, 275 (1992).
[13] J. Kersten and A. Y. Smirnov, Right-handed neutrinos at CERN LHC and the mechanism of neutrino mass generation, Phys. Rev. D **76**, 073005 (2007).
[14] E. Arganda, M. J. Herrero, X. Marcano, and C. Weiland, Imprints of massive inverse seesaw model neutrinos in lepton flavor violating Higgs boson decays, Phys. Rev. D **91**, 015001 (2015).
[15] E. Arganda, M. J. Herrero, X. Marcano, and C. Weiland, Exotic $\mu\tau jj$ events from heavy ISS neutrinos at the LHC, Phys. Lett. B **752**, 46 (2016).
[16] N. Arkani-Hamed, T. Han, M. Mangano, and L. T. Wang, Physics opportunities of a 100 TeV proton-proton collider, Phys. Rep. **652**, 1 (2016).
[17] T. Golling *et al.*, Physics at a 100 TeV pp collider: Beyond the standard model phenomena, arXiv:1606.00947.
[18] J. Baglio and C. Weiland, The triple Higgs coupling: A new probe of low-scale seesaw models, J. High Energy Phys. 04 (2017) 038.
[19] S. Antusch, E. Cazzato, and O. Fischer, Sterile neutrino searches at future e^-e^+, pp, and e^-p colliders, Int. J. Mod. Phys. A **32**, 1750078 (2017).
[20] W. Y. Keung and G. Senjanovic, Majorana Neutrinos and the Production of the Right-handed Charged Gauge Boson, Phys. Rev. Lett. **50**, 1427 (1983).
[21] A. Datta, M. Guchait, and A. Pilaftsis, Probing lepton number violation via majorana neutrinos at hadron supercolliders, Phys. Rev. D **50**, 3195 (1994).
[22] P. S. B. Dev, A. Pilaftsis, and U. K. Yang, New Production Mechanism for Heavy Neutrinos at the LHC, Phys. Rev. Lett. **112**, 081801 (2014).
[23] D. Alva, T. Han, and R. Ruiz, Heavy Majorana neutrinos from $W\gamma$ fusion at hadron colliders, J. High Energy Phys. 02 (2015) 072.
[24] C. Degrande, O. Mattelaer, R. Ruiz, and J. Turner, Fully-automated precision predictions for heavy neutrino production mechanisms at hadron colliders, Phys. Rev. D **94**, 053002 (2016).
[25] A. G. Hessler, A. Ibarra, E. Molinaro, and S. Vogl, Impact of the Higgs boson on the production of exotic particles at the LHC, Phys. Rev. D **91**, 115004 (2015).
[26] S. S. D. Willenbrock and D. A. Dicus, Production of heavy leptons from gluon fusion, Phys. Lett. **156B**, 429 (1985).
[27] D. A. Dicus and P. Roy, Supercollider signatures and correlations of heavy neutrinos, Phys. Rev. D **44**, 1593 (1991).
[28] P. S. Bhupal Dev, R. Franceschini, and R. N. Mohapatra, Bounds on TeV seesaw models from LHC Higgs data, Phys. Rev. D **86**, 093010 (2012).
[29] B. Batell and M. McCullough, Neutrino masses from neutral top partners, Phys. Rev. D **92**, 073018 (2015).
[30] A. M. Gago, P. Hernndez, J. Jones-Prez, M. Losada, and A. Moreno Briceo, Probing the type I seesaw mechanism with displaced vertices at the LHC, Eur. Phys. J. C **75**, 470 (2015).
[31] E. Accomando, L. Delle Rose, S. Moretti, E. Olaiya, and C. H. Shepherd-Themistocleous, Novel SM-like Higgs decay into displaced heavy neutrino pairs in $U(1)'$ models, J. High Energy Phys. 04 (2017) 081.
[32] M. Nemevek, F. Nesti, and J. C. Vasquez, Majorana Higgses at colliders, J. High Energy Phys. 04 (2017) 114.
[33] A. Das, P. S. B. Dev, and C. S. Kim, Constraining sterile neutrinos from precision Higgs data, Phys. Rev. D **95**, 115013 (2017).
[34] A. Caputo, P. Hernandez, J. Lopez-Pavon, and J. Salvado, The seesaw portal in testable models of neutrino masses, J. High Energy Phys. 06 (2017) 112.
[35] S. Dawson, Radiative corrections to Higgs boson production, Nucl. Phys. **B359**, 283 (1991).
[36] M. Spira, A. Djouadi, D. Graudenz, and P. M. Zerwas, Higgs boson production at the LHC, Nucl. Phys. **B453**, 17 (1995).
[37] M. Spira, QCD effects in Higgs physics, Fortschr. Phys. **46**, 203 (1998).
[38] R. V. Harlander and W. B. Kilgore, Next-to-Next-to-Leading Order Higgs Production at Hadron Colliders, Phys. Rev. Lett. **88**, 201801 (2002).
[39] V. Ravindran, J. Smith, and W. L. van Neerven, NNLO corrections to the total cross-section for Higgs boson production in hadron-hadron collisions, Nucl. Phys. **B665**, 325 (2003).
[40] S. Catani, L. Cieri, D. de Florian, G. Ferrera, and M. Grazzini, Threshold resummation at N^3LL accuracy and soft-virtual cross sections at N^3LO, Nucl. Phys. **B888**, 75 (2014).
[41] C. Anastasiou, C. Duhr, F. Dulat, F. Herzog, and B. Mistlberger, Higgs Boson Gluon-Fusion Production in QCD at Three Loops, Phys. Rev. Lett. **114**, 212001 (2015).
[42] C. Anastasiou and K. Melnikov, Pseudoscalar Higgs boson production at hadron colliders in NNLO QCD, Phys. Rev. D **67**, 037501 (2003).
[43] R. V. Harlander and W. B. Kilgore, Production of a pseudoscalar Higgs boson at hadron colliders at next-to-next-to leading order, J. High Energy Phys. 10 (2002) 017.
[44] T. Ahmed, M. Bonvini, M. C. Kumar, P. Mathews, N. Rana, V. Ravindran, and L. Rottoli, Pseudo-scalar Higgs boson production at $N^3LO_A + N^3LL'$, Eur. Phys. J. C **76**, 663 (2016).
[45] D. Binosi and L. Theussl, JaxoDraw: A graphical user interface for drawing Feynman diagrams, Comput. Phys. Commun. **161**, 76 (2004).
[46] M. Bonvini, S. Forte, G. Ridolfi, and L. Rottoli, Resummation prescriptions and ambiguities in SCET vs direct QCD: Higgs production as a case study, J. High Energy Phys. 01 (2015) 046.

[47] A. Atre, T. Han, S. Pascoli, and B. Zhang, The search for heavy Majorana neutrinos, J. High Energy Phys. 05 (2009) 030.
[48] R. Ruiz, QCD corrections to pair production of type III seesaw leptons at hadron colliders, J. High Energy Phys. 12 (2015) 1.
[49] T. Han and B. Zhang, Signatures for Majorana Neutrinos at Hadron Colliders, Phys. Rev. Lett. **97**, 171804 (2006).
[50] J. C. Collins, D. E. Soper, and G. F. Sterman, Transverse momentum distribution in Drell-Yan pair and W and Z boson production, Nucl. Phys. **B250**, 199 (1985).
[51] J. C. Collins, D. E. Soper, and G. F. Sterman, Factorization for short distance hadron-hadron scattering, Nucl. Phys. **B261**, 104 (1985).
[52] J. Collins, *Foundations of Perturbative QCD*, Cambridge Monographs on Particle Physics, Nuclear Physics and Cosmology Vol. 32, (Cambridge University Press, Cambridge, England, 2013).
[53] V. N. Gribov and L. N. Lipatov, Deep inelastic ep scattering in perturbation theory, Yad. Fiz. **15**, 781 (1972) [Sov. J. Nucl. Phys. **15**, 438 (1972)].
[54] Y. L. Dokshitzer, Calculation of the structure functions for deep inelastic scattering and e^+e^- annihilation by perturbation theory in quantum chromodynamics, Zh. Eksp. Teor. Fiz. **73**, 1216 (1977) [Sov. Phys. JETP **46**, 641 (1977)].
[55] G. Altarelli and G. Parisi, Asymptotic freedom in parton language, Nucl. Phys. **B126**, 298 (1977).
[56] T. Becher and M. Neubert, Threshold Resummation in Momentum Space from Effective Field Theory, Phys. Rev. Lett. **97**, 082001 (2006).
[57] T. Becher, M. Neubert, and B. D. Pecjak, Factorization and momentum-space resummation in deep-inelastic scattering, J. High Energy Phys. 01 (2007) 076.
[58] S. Catani and L. Trentadue, Resummation of the QCD perturbative series for hard processes, Nucl. Phys. **B327**, 323 (1989).
[59] G. F. Sterman, Summation of large corrections to short distance hadronic cross-sections, Nucl. Phys. **B281**, 310 (1987).
[60] S. Catani and L. Trentadue, Comment on QCD exponentiation at large x, Nucl. Phys. **B353**, 183 (1991).
[61] H. Contopanagos, E. Laenen, and G. F. Sterman, Sudakov factorization and resummation, Nucl. Phys. **B484**, 303 (1997).
[62] S. Forte and G. Ridolfi, Renormalization group approach to soft gluon resummation, Nucl. Phys. **B650**, 229 (2003).
[63] C. W. Bauer, S. Fleming, D. Pirjol, and I. W. Stewart, An effective field theory for collinear and soft gluons: Heavy to light decays, Phys. Rev. D **63**, 114020 (2001).
[64] C. W. Bauer, D. Pirjol, and I. W. Stewart, Soft collinear factorization in effective field theory, Phys. Rev. D **65**, 054022 (2002).
[65] M. Beneke, A. P. Chapovsky, M. Diehl, and T. Feldmann, Soft collinear effective theory and heavy to light currents beyond leading power, Nucl. Phys. **B643**, 431 (2002).
[66] T. Becher, M. Neubert, and G. Xu, Dynamical threshold enhancement and resummation in Drell-Yan production, J. High Energy Phys. 07 (2008) 030.
[67] V. Ahrens, T. Becher, M. Neubert, and L. L. Yang, Renormalization-group improved prediction for Higgs production at hadron colliders, Eur. Phys. J. C **62**, 333 (2009).
[68] C. F. Berger, C. Marcantonini, I. W. Stewart, F. J. Tackmann, and W. J. Waalewijn, Higgs production with a central jet veto at NNLL + NNLO, J. High Energy Phys. 04 (2011) 092.
[69] T. Ahmed, T. Gehrmann, P. Mathews, N. Rana, and V. Ravindran, Pseudo-scalar form factors at three loops in QCD, J. High Energy Phys. 11 (2015) 169.
[70] V. Ahrens, A. Ferroglia, M. Neubert, B. D. Pecjak, and L. L. Yang, RG-improved single-particle inclusive cross sections and forward-backward asymmetry in $t\bar{t}$ production at hadron colliders, J. High Energy Phys. 09 (2011) 070.
[71] A. Broggio, A. Ferroglia, B. D. Pecjak, A. Signer, and L. L. Yang, Associated production of a top pair and a Higgs boson beyond NLO, J. High Energy Phys. 03 (2016) 124.
[72] M. Bonvini and L. Rottoli, Three loop soft function for N^3LL' gluon fusion Higgs production in soft-collinear effective theory, Phys. Rev. D **91**, 051301 (2015).
[73] R. V. Harlander, Virtual corrections to $gg \to H$ to two loops in the heavy top limit, Phys. Lett. B **492**, 74 (2000).
[74] A. Idilbi, X. d. Ji, and F. Yuan, Resummation of threshold logarithms in effective field theory for DIS, Drell-Yan and Higgs production, Nucl. Phys. **B753**, 42 (2006).
[75] F. Caola and S. Marzani, Finite fermion mass effects in pseudoscalar Higgs production via gluon-gluon fusion, Phys. Lett. B **698**, 275 (2011).
[76] R. D. Ball *et al.* (NNPDF Collaboration), Parton distributions for the LHC run II, J. High Energy Phys. 04 (2015) 040.
[77] R. D. Ball, V. Bertone, S. Carrazza, L. Del Debbio, S. Forte, A. Guffanti, N. P. Hartland, and J. Rojo (NNPDF Collaboration), Parton distributions with QED corrections, Nucl. Phys. **B877**, 290 (2013).
[78] K. A. Olive *et al.* (Particle Data Group), Review of particle physics, Chin. Phys. C **38**, 090001 (2014).
[79] M. Bonvini, S. Marzani, J. Rojo, L. Rottoli, M. Ubiali, R. D. Ball, V. Bertone, S. Carrazza, and N. P. Hartland, Parton distributions with threshold resummation, J. High Energy Phys. 09 (2015) 191.
[80] T. Hahn, CUBA: A library for multidimensional numerical integration, Comput. Phys. Commun. **168**, 78 (2005).
[81] M. Bonvini and S. Marzani, Resummed Higgs cross section at N^3LL, J. High Energy Phys. 09 (2014) 007.
[82] M. Mitra, R. Ruiz, D. J. Scott, and M. Spannowsky, Neutrino jets from high-mass W_R gauge bosons in TeV-scale left-right symmetric models, Phys. Rev. D **94**, 095016 (2016).
[83] W. Beenakker, C. Borschensky, M. Krmer, A. Kulesza, E. Laenen, S. Marzani, and J. Rojo, NLO + NLL squark and gluino production cross-sections with threshold-improved parton distributions, Eur. Phys. J. C **76**, 53 (2016).
[84] A. Buckley, J. Ferrando, S. Lloyd, K. Nordstrm, B. Page, M. Rfenacht, M. Schnherr, and G. Watt, LHAPDF6: Parton density access in the LHC precision era, Eur. Phys. J. C **75**, 132 (2015).